Analysis and Discussion of a Concept for an Adjustable Inductance Based on an Impact of an Orthogonal Magnetic Field

Guido Schierle, Michael Meissner, Klaus F. Hoffmann
HELMUT SCHMIDT UNIVERSITY
UNIVERSITY OF THE FEDERAL ARMED FORCES HAMBURG
Holstenhofweg 85
22043 Hamburg, Germany
Tel.: +49 / (0)40 6541 2768
Fax: +49 / (0)40 6541 2018
Email: guido.schierle@hsu-hh.de
URL: https://www.hsu-hh.de/lek/en/

Keywords

≪Coupled inductor≫,≪Passivity≫, ≪Passive component≫, ≪Passive component integration≫, ≪Magnetic coupling≫, ≪Magnetic device≫, ≪Winding topology≫.

Abstract

In this paper the realisation of a concept for an adjustable inductance by the use of an auxiliary control current is analysed and discussed. Using a construction of two magnetic toroid cores the magnetic field of a load core, and by this its effective inductance, is influenced by an orthogonal magnetic field induced by an additional control core. It will be shown that with an increase of the magnetic field generated by the control circuit the inductance of the load circuit decreases.

Introduction

Inductors are essential components for power electronic applications. Their effective inductivity mainly depends on the number of turns of a winding and, when using a core, the geometry and the characteristics of the used material. Therefore, an influence on the effective inductance of an electric circuit apart from an adjustment of the number of turns or the core itself needs to be achieved otherwise. In this paper one of various concepts for adjustable inductances is presented and analysed [1, 4, 5, 6]. In the past, current-controlled inductors were used for many applications, e.g. for AC power control or special gate drivers [2, 4, 5]. The motivation for this extended investigation is a possible integration of the described principle in e.g. resonant converters with high switching frequencies and a power range of 2-50 kW. An adjustable inductor would allow to control both the resonant frequency and the characteristic impedance of the resonant tank, in addition to the widely used parameter of switching frequency.

Inductive core setup

The objective of the below described setup (Fig.1) is to achieve a controllability on the effective inductance during operation. Therefore, a magnetic field orthogonal to the magnetic field of the load inductance will be used. The inductive core setup is comprised on the one hand by a winding around a magnetic core, the load core. On the other hand, another magnetic toroid core, in the following named control core, is implemented perpendicularly. Fig. 1 depicts the theoretical setup of the orthogonal circuit. It also shows that the control circuit provides a DC current. Following from this the control core is permeated with a constant magnetic flux. It can be seen that the resulting magnetic field of the control core in an idealized construction should be orthogonal to the magnetic field of the load core. In the area of the shared volume there will be a resulting magnetic flux, with an orientation depending on the strength of both magnetic fields.

For construction, a segment of the control core was removed according to the dimensions of the load core. This ensures the area of the control core which is implemented onto the load core fits as tightly

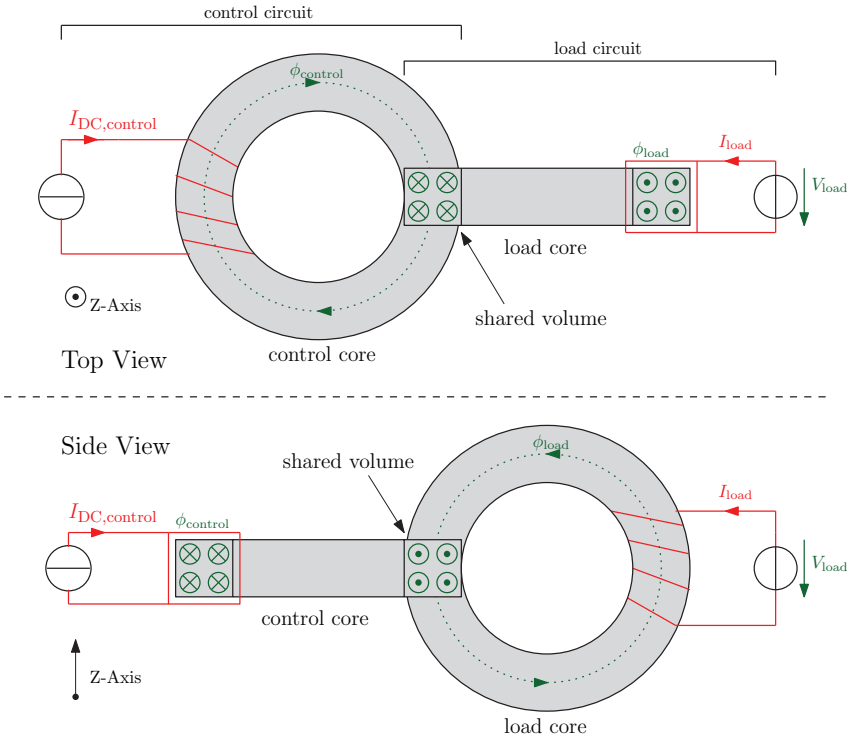

Fig. 1: Design of the orthogonal connection of load and control core [8]

as possible to minimize the resulting parasitic air gap. Fig. 2a presents a prototype of the theoretical setup. For better visualisation the load and the control core of the first setup are marked. The core in the background will be used for investigations regarding the influence of the size of the shared volume and is made from the same material as the bigger core. From the construction of the inductive core setup a simplified magnetic circuit was derived and is presented in Fig. 2b. The magnetic resistance $R_{\text{m,shv}}$ describes the reluctance of the shared volume of both cores. The magnetic resistances $R_{\text{m,air}}$ depicts the reluctance of the parasitic air gap.

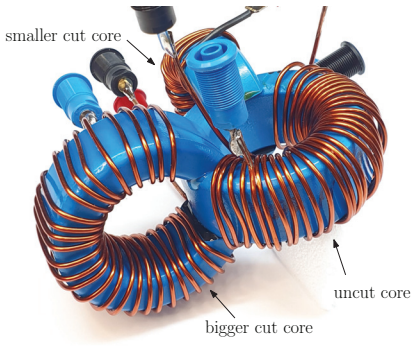

(a) Prototype of the orthogonal connection

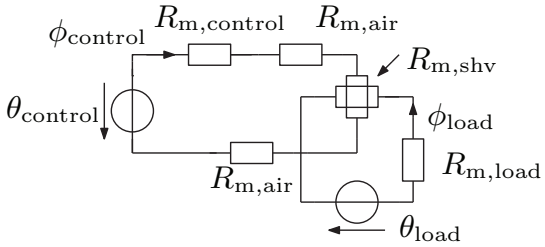

(b) Resulting magnetic circuit

Fig. 2: Prototype of the orthogonal connection of load and control core with resulting magnetic circuit

The impact of the air gap will be examined and discussed in this paper. Therefore, both cores will be swapped in their function, which means that the cut core will be used as the load and the uncut core will operate as the control core.

This concept for a current-controlled inductance was chosen because of two reasons. First, Fig. 1 shows that the influence of the control core can be limited to a specific area of the load core, depending on the size of the control core. Second, following the assumption that both magnetic fields are orthogonal to each other the magnetic field of the load core should not affect the magnetic flux of the control core beyond the shared volume. According to Faraday's Law no voltage is induced in the control circuit so that the used power source is protected, which could differ from other concepts of current-controlled inductors [3, 4, 9].

The control core

The magnetic field of the control core shall influence the effective inductance of the load core. Therefore, magnetic fundamentals will be described in the following.

Simplified, a constant and homogeneous magnetic flux density in the magnetic cross section is assumed and stray fields are neglected. Considering the described simplifications and Ampère's circuital law (displacement currents are not taken into account) the magnetic field strength and the current in the winding are related as equation (1) shows [7].

$$\theta = \oint \vec{H}(t)\, d\vec{l} = \sum_n H_n(t) \cdot l_{\mathrm{e},n} = N \cdot i(t) \tag{1}$$

For an impact of the control core on the load core an according magnetic field strength is needed. One additional requirement for the analysis is the saturation of the control core and therefore the saturation of the shared volume of both cores during fixed operating points. Here, it should be considered that in the parasitic air gap, resulting from construction, magnetic energy is stored [3]. Hence, a higher magnetic field strength, and for this reason a higher number of turns of the winding N and/or a higher current I is needed to saturate the core as equation (1) clarifies. Using a defined core the effective magnetic path length l_e remains constant. Regarding the used steps of control current the number of turns of the control winding were defined and remained constant.

Measurement method

The load voltage of Fig. 1 was generated by the Power Choke Tester DPG 20. To determine the effective inductance the Choketester applies a pulsed measurement method. At the beginning of the measurement a capacitor bank is charged and afterwards a square wave DC voltage is applied to the DUT. The current in the load circuit starts to rise with a slew rate, dependent on the inductance L, which is also a function of the current. As soon as a pre-defined maximum current is reached, the measurement ends. Since this measurement device has a maximum of 100 sampling points the simplified equation (2) is used to calculate the inductance. According to the equation it can be calculated by the time interval for the rise of current with an almost constant voltage. Further information to the measurement method are given in [10].

$$v_\mathrm{L}(t) = L \cdot \frac{\triangle i(t)}{\triangle t} \tag{2}$$

A distinction is made between incremental inductance L_inc and secant inductance L_sec. The incremental inductance describes the tangent at an operating point for a small modulation. However, L_sec is defined by a secant between an operating point and the origin. Especially during saturation of the core material, the values show significant differences. For power electronic applications often the currently effective inductance L_inc is of interest. Thus, only the incremental inductance will be analysed [7].

Additionally, the Choketester was used to examine the magnetic flux density. Because of the saturation of the shared volume it is expected that it behaves like an air gap or more specifically the magnetic reluctance should increase for the load core. For this reason, a higher magnetic field strength is needed to reach the same magnetic flux density in the load core as without the impact of the control core. Hence, the *B-H* characteristic of the inductance of the load core should decrease with increasing control current.

The flux linkage $\Psi(i)$ is calculated as the product of the inductance, given by equation (2), and the current as equation (3) shows, which is equivalent to the the product of the number of turns N and the magnetic flux Φ .

$$\Psi(i) = L(i) \cdot i = N \cdot \Phi \tag{3}$$

With information about the number of turns and the effective magnetic cross section A_e the Choketester calculates the magnetic flux density B using the equation (4).

$$B = \frac{\Psi}{A_\mathrm{e} \cdot N} \tag{4}$$

The calculation used is sufficiently accurate for a general analysis of the concept. The results of the inductance of the load core and the *B-H* characteristics are presented and discussed hereinafter.

Measurement results

Based on the rising control current the different characteristics of the incremental inductance L_{inc} and the magnetic flux density of the load core are depicted and interpreted. For the load circuit the Choketester was configured to stop the measurement once the load current reaches 11 A, because it was observed in earlier measurements that the load core was almost entirely saturated at this value.

Impact of the control current on differential inductance

The steps of the control current were chosen to follow the E-12 series. After a first analysis of the measurement results some current steps were added in order to fill occurring gaps, because a relatively significant decrease in the effective inductance was detected. The maximum value was defined to 100 A. The results of the measurement with different control currents are shown in Fig. 3.

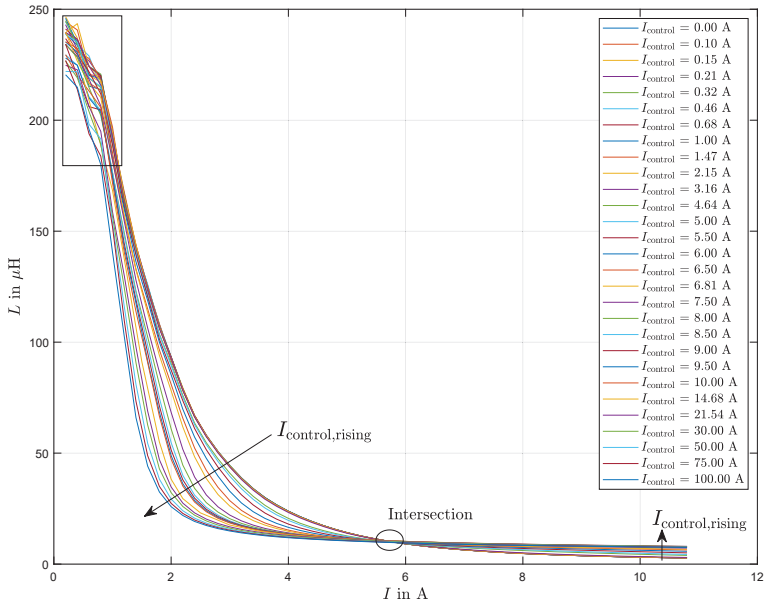

Fig. 3: Dependency of the effective inductance to the applied control current

Fig. 3 presents that the load core saturates increasingly with a rising load current right from the start of the measurement even when there is no control current applied. Because of measurement inaccuracies at low currents, indicated by a rectangle in the top left corner, the results of the beginning of the curves are not taken into account for analysis.

Clearly, it can be seen that the incremental inductance decreases from the beginning of the analysed measurement with a rising control current. With no control current the effective inductance has a value of about 90 µH at a load current of 2 A. With rising control current the effective inductance decreases down to a value of around 35 µH at a control current of 30 A and 25 µH for 100 A. The drop of effective inductance between the step of control current from 21.54 A to 30 A or even from 50 A to 100 A is significantly smaller than between 4.64 A and 6.81 A although the absolute increase in control current is obviously higher, justifying the chosen E-12 series for the values. It is noticeable, that all measurement curves intersect in the area of a load current around 5.7 A. In the following this intersection will be examined more closely. The area of intersection is indicated by an ellipse in Fig. 3. From the point of intersection, it can be observed that the effective inductance decreases more slowly with increasing control current. The magnetic domain of a ferrite core could provide an explanation for this behaviour. The rising control current generates a magnetic field in the shared volume of both cores. Due to an increase in the load current the resulting magnetic field in the shared volume aligns more and more in the direction of the magnetic field of the load core. To verify this assumption, the impact of the size of the shared volume and therefore the area in which both magnetic fields are superpositioned will be investigated further. Additionally, the ratio of the magnetic field of the load core and the magnetic field of the control core will be varied by increasing the number of turns of the load core.

Investigation of the size of the shared volume

In order to investigate the influence of the size of the shared volume a smaller control core, made of the same material, was implemented similar to the bigger core. The final setup is shown in Fig. 2a with the smaller control core in the background. To obtain equally effective magnetic fields for both cores the same magnetic field strength needs to be achieved. For this reason and in due consideration of equation 1, assuming the same length of air gaps, the number of turns for the smaller core was chosen accordingly.

Subsequently, the setup was operated with the smaller core as control core. For better visualization, the used control current was limited to 30 A and only chosen values are presented. Fig. 4a shows the influence on the differential inductance of both, the bigger and the smaller control core.

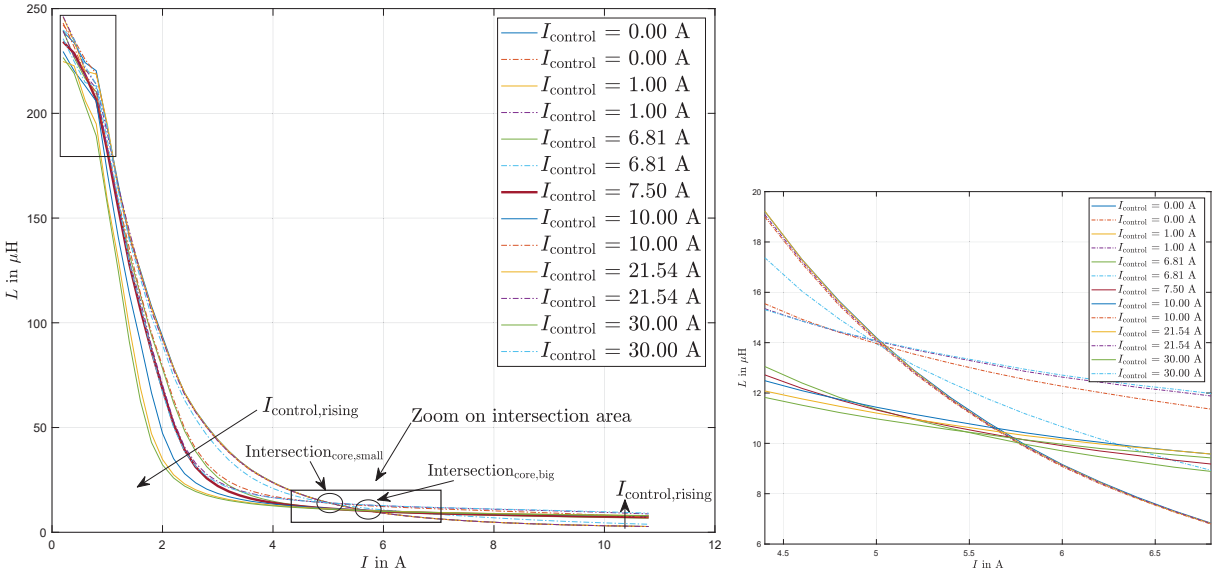

(a) Comparison of impact of size of shared volume. Dotted lines represent the smaller control core, solid lines the bigger control core

(b) Zoom on both intersection areas from Fig. 4a

Fig. 4: Impact of the size of shared volume with focus on both intersection areas

The comparison of the measurement curves shows that a larger shared volume has a greater impact on the differential inductance, especially at the beginning of the measurement around 2 A. While the smaller core starts to have a slight influence on the differential inductance (first dotted light blue curve) at a control current of 6.81 A the bigger core already lowered the effective inductance from around 90 µH to about 75 µH with the same current (first solid green curve). For 30 A, the maximum of the applied control current, the difference is even more significant. The inductance decreases from the initial 90 µH to around 70 µH for the smaller control core but only has a value of around 30 µH for the bigger core. The curves converge with rising load current and therefore the differences between the cores drop. It is conspicuous that both cores have an intersection area but the curves of the smaller core intersect with a lower load current and for this reason a higher effective inductance. After the intersection point the curves only drop slightly with increasing load current. For a control current of 21.54 A and 30 A regarding the smaller core the effective inductance still has a greater value in comparison to the bigger core. However, the curves show a larger negative slope which is hard to see in the figure but could be observed for all measurements with higher load currents. The bigger the core and the higher the control current the lower was the negative slope of the respective differential inductance after the intersection area. This behaviour could be addressed in further investigations.

To outline the opportunity of a possible trade-off between the size of the shared volume and the applied control current an additional measurement with 7.5 A, using the bigger core as control core, was added to fig. 4a and is represented by the dark red solid line. It is noticeable that right from the start until a load current of 2.5 A is reached, the effective inductance of the load core shows similar behaviour. It is influenced by the bigger core with a control current of 7.5 A and by the smaller core with a control current of 30 A. With rising load currents both graphs split but the curve for 30 A of the smaller control

core intersects exemplarily with the curve for 6.81 A of the bigger control core. This illustrates that nearly every desired operating point of the effective inductance could be reached, varying the size of the shared volume or adapting the control current correspondingly. Future examinations should focus on the influence of possible differences of the length of the airgap resulting from construction.

Fig. 4b shows a selected area around the intersection from Fig. 4a. The dotted lines represent the smaller core and the solid lines the bigger core. The figure depicts that the measurement curves of the smaller control core intersect with a lower load current of about 5 A. Furthermore, the effective inductance dropped to a value of 14 µH. For the bigger core the intersection of the curves with an applied control current and the one with no control current occur in an area from 5.6 A - 5.75 A. The effective inductance for the chosen curves varies only slightly from nearly 11 µH to 10 µH at the respective intersection point. It can be derived that the larger the magnetic field of the load core in ratio to the magnetic field of the control core the less load current is needed to reach the intersection area.

Impact of the ratio of the magnetic fields on differential inductance

The influence of the magnetic field generated by the load current should be examined more closely to test its influence on the intersection area. To obtain a higher magnetic field strength and therefore a higher magnetic flux density, the number of turns on the load side was raised, according to equation 1. The range of the load current and the magnetic path length remained constant. Based on the previous results, it can be presumed that following from the higher magnetic field of the load side the measurement curves of the differential inductance should intersect with a smaller load current.

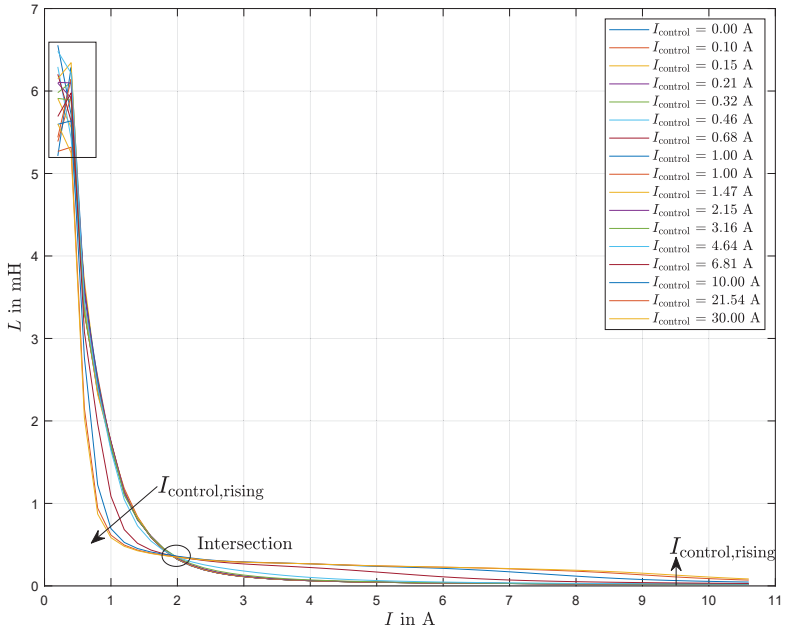

Fig. 5: Influence of the magnetic field of the load core on intersection area

Fig. 5 shows the results of the measurement with control currents up to 30 A. It can clearly be seen that with a rising control current the effective inductance decreases, as in case of the investigation with a lower number of turns. The change of the intersection area is visible distinctly, changing from 5.8 A with a lower number of turns to about 2 A with a higher number of turns.

It can be derived that the intersection area depends strongly on the ratio of the magnetic field of the load core and the magnetic field of the control core, because both magnetic fields are superpositioned in the area of the shared volume. The stronger the magnetic field of the load core the earlier the measurement curves of the differential inductance will intersect. An explanation could be found in the magnetic domains of the core material. Due to the magnetic field of the control side the Weiss domains of the shared volume are magnetized corresponding to the direction of the magnetic flux. For this reason, the magnetic resistance of the shared volume rises and the total reluctance of the magnetic circuit of the load core increases. With the same magnetomotive force of the load core a higher magnetic resistance

leads to a lower magnetic flux and therefore the effective inductance decreases, which is observable in the previous measurement curves [3]. The premagnetized Weiss domains need to be aligned in the direction of the magnetic flux of the load core. With rising load currents the magnetic field of the load core increases and will dominate the superposition of the magnetic fields in the shared volume, because the Weiss domains will align more and more in the direction of the magnetic flux of the load core.

Trade-off number of turns vs control current

As already explained, there is a trade-off between the size of the shared volume and the control current. Regarding the efficiency for a possible implementation in an electrical circuit another degree of freedom is examined. Because of the dependency of the magnetic field on the magnetic field strength and therefore on the number of turns and the current of the control core, it is investigated if the number of turns and the current can be balanced equally.

Equation 5 presents the possible trade-off between the number of turns and the current. The index describes the number of turns. Even if the factors vary, the magnetic field strength still has to have the same value to generate the same magnetic field. Hence, the influence of the control core on the effective inductance of the load core should only be dependent on the ratio of the number of turns multiplied with the current. The equation clarifies that a needed current can be substituted with a higher number of turns.

$$\begin{aligned} H_{N27} = H_{N22} = \frac{N_{27} \cdot I_{27}}{l_e} = \frac{N_{22} \cdot I_{22}}{l_e} \\ I_{27} = \frac{N_{22}}{N_{27}} \cdot I_{22} \end{aligned} \tag{5}$$

For exemplary values the results of this verification by measurement are observable in fig. 6.

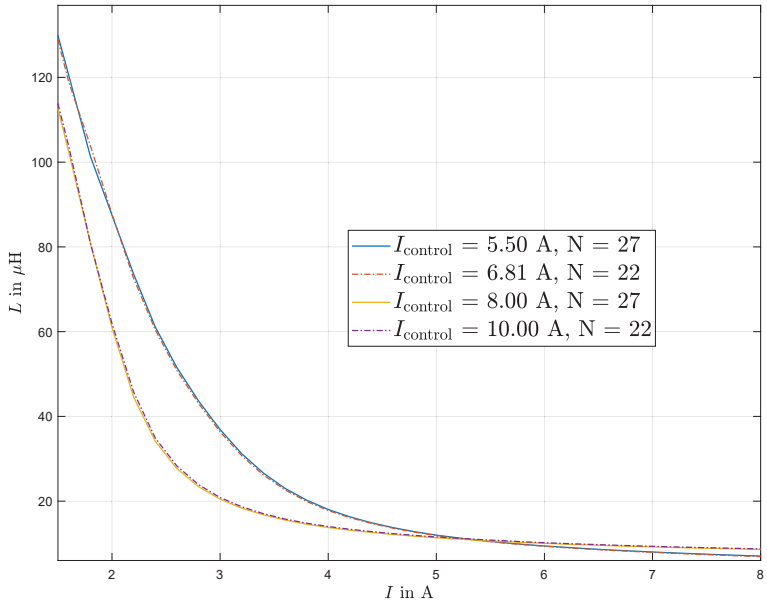

Fig. 6: Trade-off between control current and number of turns for the load core

The outcomes illustrate that the number of turns and the control current can be exchanged using equation 5. Considering that for the electrical losses the current is squared and the ohmic resistance, which increases with a higher number of turns, is taken into account only linearly a sensible trade-off can be found. Together with the size of the shared volume there are three degrees of freedom which can influence the efficiency of a system using this setup. However, according to Faraday's Law the higher number of turns on the control core could lead to a disadvantage regarding the magnetic back coupling of the system on the control circuit. Though, as described in the inductive core setup, this construction was chosen because both magnetic fields are orthogonal and therefore should not affect each other beyond the shared volume. This needs to be investigated further in the future to clarify its influence on a possible realization of the setup for application in an electrical circuit and to find potential limits of the trade-off.

Swap of control and load core in their function

As explained in the inductive core setup there will be a parasitic air gap resulting from construction. To examine its influence the setup will be reversed, so that the uncut core will work as the control core and the bigger cut core as the load core. The resulting magnetic circuit is shown in fig. 7b. This means that independent of the applied control current an air gap already exists in the load circuit. For this reason the load current was increased to the devices technical maximum value of 100 A to ensure a saturation of the load core [11]. For additional comparison the effective inductance of the cut core with pure air gap and thus without the implementation of the uncut core was measured for reference. The results are depicted in fig. 7a. The horizontal blue curve which has a value of a around 4.5 µH represents the measurement with no core implemented, so with a pure and because of this a relatively ”big” air gap. It displays that there is no saturation at all without the implementation of the uncut core for the chosen parameters.

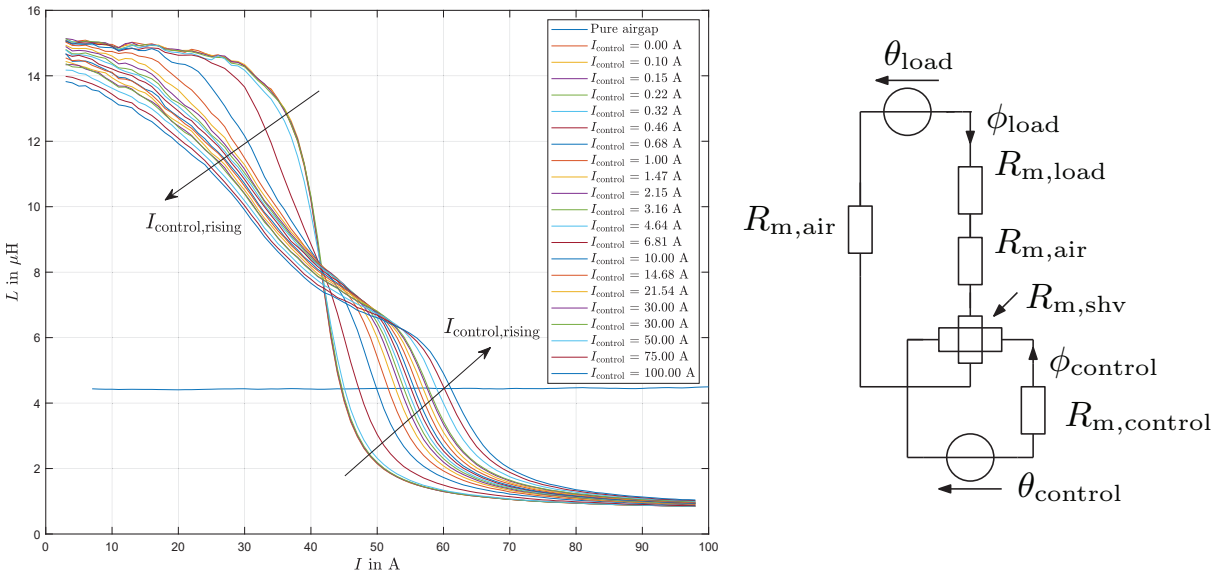

(a) Dependency of inductance to applied control current for swapped cores (b) Resulting magnetic circuit for swapped cores

Fig. 7: Dependency of the effective inductance with swapped cores with corresponding magnetic circuit

The green and purple curve representing 30 A are introduced for comparison, because for the higher currents another current source was used. Both validate that the effect on the differential inductance is sufficiently enough the same. With no control current applied the effective inductance shows the characteristic behaviour of an inductance with a small air gap compared to the state when no core is implemented. The inductance remains constant until a load current of 30 A is reached. At higher values the core starts to saturate, the permeability decreases and therefore the value of the inductance drops rapidly to an almost constant value for which the core is saturated completely [3]. It is visible that the reached constant value is smaller than for measurement with pure air gap. This behaviour should be adressed further, an explanation could be the widening of the air gap. This widening leads to a larger magnetic cross section A_e, therefore to a lower magnetic flux density as equation 4 shows and because of this to a larger value of the effective inductance as equation 3 clarifies [3].

Beyond that, fig. 7a depicts that with rising control current the effective inductance decreases. Complementary to the previous setup a comparatively small control current of 0.46 A (first dark red line) already has an noticeable impact on the effective inductance. Furthermore, the effective inductance decreases right from the start and does not remain constant with increasing control current. The decline of the measurement curves kind of linearize until the point of sudden saturation is reached. Following from this, the setup should be taken into consideration for realizations of the concept, especially concerning a required closed loop control, which would be needed to adjust the inductance based on the requirements of the load side. Additionally, the typical sharp decline because of the saturation of the core happens with a higher load current and with a smaller negative slope. The absolute drop of the effective inductance from the point of sudden saturation lowers with rising control current as well. Finally, there is an intersection

area visible, too. It can been seen that with rising control currents the curves intersect at a lower effective inductance and with a slightly higher load current, which supports the previous assumptions.

In order to verify the earlier described effect of the ratio of both magnetic fields and to show that larger, reasonable values of effective inductance can be reached the number of turns of the load core was increased. The results are presented in fig. 8a.

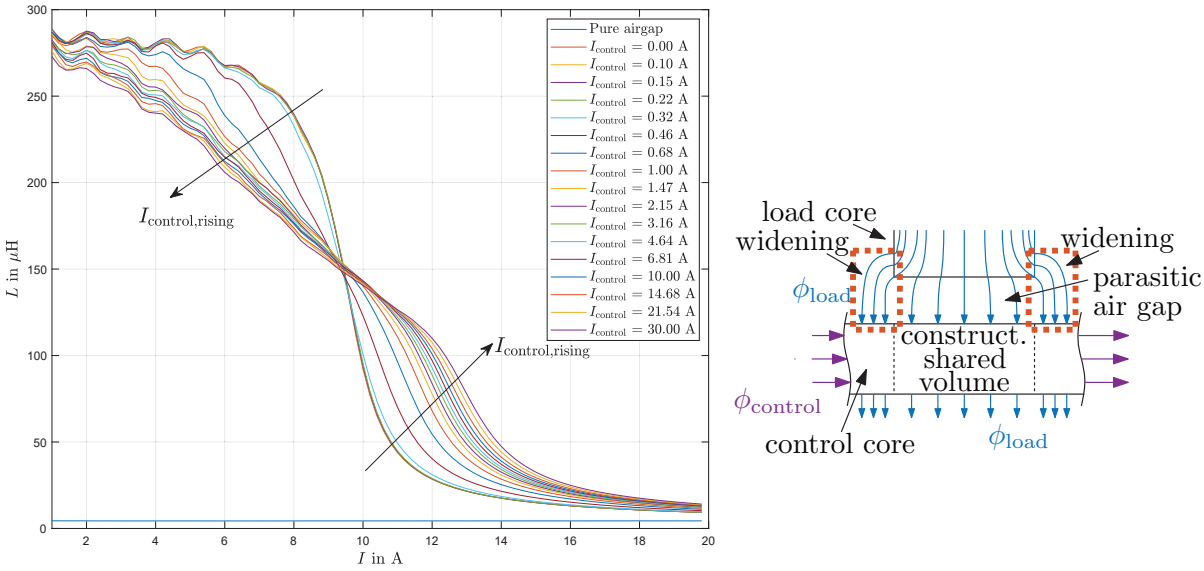

(a) Dependency of the effective inductance on ratio of magnetic fields

(b) Widening of the air gap

Fig. 8: Dependency of inductance on higher ratio of magnetic fields and resulting widening of air gap

According to the results from previous examination the curves intersect at a significantly lower load current. As observed in the examination with a lower number of turns, the higher the control current the higher is the needed load current to intersect the respective curve with the initial one and the lower is the effective inductance. The effective inductance of the pure air gap was added to the figure as reference like in the examination before. It is observable that the saturated inductances does not have the same values as the one with pure airgap or with a lower number of turns. An explanation could be found in the widening of the air gap of the load core following from the increase of number of turns. In contrast to the pure air gap the magnetic flux can permeate more permeable material of the control core, because of the widening, which is symbolized in fig. 8b. This leads to larger values of the effective inductance.

Corresponding to the slope of the decrease of the effective inductance this setup seems to be promising showing less variation in the inductance-value with small changes of the load current. Nevertheless, the effective inductance could be varied for this example at a load current of 6 A from 270 µH to 210 µH, giving a large range of different values realizable.

Impact of the control current on $B-H$ characteristic

It was anticipated that the shared volume would behave like a variable air gap. To verify that, the magnetic flux density is plotted against the load current. To show the basic effect on the $B-H$ characteristic, the setup and the according results of the measurement presented in fig. 3 were used. The magnetic field strength could be used instead of load current but regarding equation (1) the number of turns and the effective magnetic path length are constant and therefore only a proportionality factor would scale the measurement curves shown in fig. 9.

This shows that with an increase in control current the $B-H$ characteristics starts to flatten. The slope of the curves decreases with rising control currents for lower load currents. Thus, a higher magnetic field strength is aquired to reach the same magnetic flux density. Moreover, it can be seen for further rising load currents, that the slope of the curves start to behave contrary, because of the saturation of the core. From this point on, the slope approximates to the vacuum permeability. Furthermore, with increasing control current the curvature of the $B-H$ characteristics decreases. Consistent to the results presented in fig. 3 the first noticeable influence can be observed for a control current of 4.64 A.

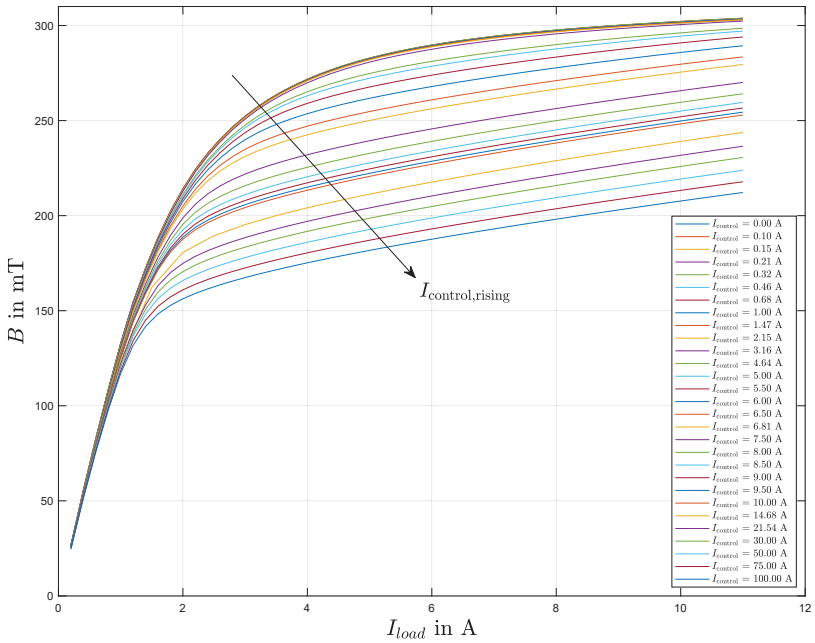

Fig. 9: *B-H* characteristics for an increase in control current

Conclusion and prospective

This paper presents a concept for an adjustable inductance by the use of a control current. A decrease of the effective inductance with an increase in control current was clearly observable in the measurement curves. As expected, the corresponding $B-H$ characteristics flatten. It was outlined that the ratio of the magnet fields of load and control core are essential for the intersection area. Furthermore, degrees of freedom were explained and therefore possibilities of optimization were derived concerning the efficiency of the system.

In future investigations the magnetic back coupling on the control circuit, the usage of several control cores at once, AC current on the load side and different materials will be analysed. Generally, a closed loop control needs to be implemented for realization, which adjusts the control current. A mathematical approach to calculate the influence on the effective inductance should be a target to derive control parameters. Otherwise, the measured change of the current in the inductivity and the measured voltage must be used as feedback. Additionally, the results of the measurements should be verified with another method to examine systematical and statistical errors using the Choketester measurement.

References

[1] E. S. Tez : ”The Parametric Transformer”. PhD Thesis, Loughborough University of Technology, 1977

[2] F. Kümmel: ”Regel-Transduktoren. Theorie und Anwendungen in der Regelungstechnik”. Springer, 1961

[3] M. Albach: ”Induktivitäten in der Leistungselektronik. Spulen, Trafos und ihre parasitären Eigenschaften”. Springer Vieweg, 2017

[4] J. P. Karst, K. Hoffmann, ”Design Rules for Transductor based Gate Drives”. Power Conversion and Intelligent Motion Conference-PCIM , 2005

[5] J. P. Karst, K. Hoffmann, ”Transductor based high speed gate drive”. 2004 IEEE 35th Annual Power Electronics Specialists Conference, 2004

[6] J. P. Karst, K. Hoffmann, ”High Speed Complementary Gate Drives Utilising a Single Planar Transformer”. Power Conversion and Intelligent Motion Conference-PCIM, 2004

[7] S. Fahlbusch: ”Messsystem zur Charakterisierung von Leistungsspulen auf Basis eines 15-Level-Siliziumkarbid-Wechselrichters”. PhD Thesis, Helmut Schmidt University, 2020

[8] D. Magel: ”Implementation, Analysis and Comparison of Different Prototypes of Current Controlled Inductors for Power Electronic Applications”. Bachelor Thesis, Helmut Schmidt University, 2022

[9] S. Brandt, M. Meissner, N. Polap, G. Schierle, K. F. Hoffmann: ”A Survey on Adjustable Inductances for Power Electronic Circuits”. PCIM Europe digital days 2022, 2022

[10] H. Kreis: ”Pulsed Inductance Measurement on Magnetic Components from 0.1A to 10kA.”, in Bodos Power Systems, Nov 2021

[11] ed-k: ”Power Choke Tester DPG10 B - Serie & DPG 20. Manual”. 01/2020